Chapter 7

COARSENING

In the previous chapter, we discussed the dynamics of discrete spin systems. Our primary focus was on a prototypical system that is initially in a homogeneous high-temperature disordered phase and the temperature is quenched (suddenly lowered) to below the critical temperature. Because of the complexity of this domain coarsening process at the level of discrete spins (see Fig. 6.7), considerable effort has been devoted to constructing a complementary approach that is based on a phenomenological description at the continuum level. There are many motivations for going to a continuum description. While we lose a direct connection to the individual degrees of freedom of the system in a continuum description, continuum theories are typically simpler than their discrete counterparts. This simplification is particularly important in coarsening phenomena because continuum theories are still quite formidable.

When a homogeneous system is quenched to below the critical temperature, a coarsening mosaic of ordered-phase domains forms, as the distinct broken-symmetry phases compete with each other in their quest to select the low-temperature thermodynamic equilibrium state. As a result of this competition, equilibrium is never reached for an infinite system. Instead, self-similar behavior typically arises, where the domain mosaic looks the same at different times but only its overall length scale changes. This self-similarity is an important simplifying feature that is characteristic of coarsening.

In this chapter, we will investigate some of the simplest manifestations of coarsening. We will solve the basic bidiffusion equation that describes coarsening in the TDLG equation. We will particularly emphasize systems whose initial state are sufficiently simple that the resulting interface dynamics can be obtained explicitly. Examples of such system include a droplet of one phase that is immersed into another phase, or a single domain wall, so that the domain geometry remains simple throughout the coarsening. For such cases, a complete solution for the evolution can sometimes be found. For the more generic case of a random initial condition, the continuum approach provides many new insights that seem to be impossible to obtain by a description at the level of individual spins.

7.1 The Models

We shall tacitly assume that the order parameter is a scalar; otherwise, we will explicitly state its nature. It is helpful to keep in mind the concrete example of magnetic systems, and we often use the terminology associated with magnetic systems. However, this usage is more reflective of tradition rather than the dominant application of coarsening. Even for the simplest case of systems with a scalar order parameter, there is a choice between the microscopic and the macroscopic descriptions, as mentioned above, between non-conservative (Landau-Ginzburg) and conservative (Kawasaki) dynamics, *etc.* The distinction between conservative and non-conservative dynamics is crucially important and we now outline the two generic models of these dynamics.

Non-conservative dynamics

The three basic ingredients that underlie non-conservative Landau-Ginzburg dynamics are the following:

- We treat the order parameter (for example, the magnetization for magnetic systems) as a continuous function $m(\mathbf{x},t)$ rather than a binary Ising variable $\sigma=\pm1$. We define this coarse-grained magnetization as $m(\mathbf{x},t)\equiv \ell^{-d}\sum\sigma$; namely, the average magnetization in a block of linear dimension ℓ, where the sum runs over the ℓ^d spins in the block centered at $\mathbf{x}$. Here ℓ should be much greater than the lattice spacing a and much smaller than the system size $\mathcal{L}$. These restrictions lead to a magnetization that varies smoothly on a scale greater than ℓ and that can account for a non-trivial spatial dependence. This coarse graining should be appropriate over the time range where the typical domain size is much larger than ℓ and much smaller than $\mathcal{L}$.

- We describe the thermodynamics of the system by the coarse-grained Landau free-energy functional

$$F[m]=\int d\mathbf{x}\left[\frac{1}{2}\,|\nabla m|^2+V(m)\right], \tag{7.1}$$

  where the potential $V(\phi)$ has a double-well structure with minima corresponding to the equilibrium states. (The standard example is $V(m)=\frac{1}{2}\,(1-m^2)^2$; for systems with two degenerate minima, we always assume that the minima occur at $m=\pm1$ and $V(\pm1)=0$.) While this coarse-grained free energy is intuitively plausible—it combines the Landau mean-field theory with the lowest order contribution due to spatial variation of the order parameter—it is not possible to derive Eq. (7.1) from first principles starting with a microscopic model, such as the Ising model.

- The final step in constructing a coarse-grained dynamical description is also phenomenological: we simply assert that the order parameter changes at a rate that is proportional to the local thermodynamic force $\delta F/\delta m(\mathbf{x},t)$. Thus that we are considering *overdamped* dynamics. This assumption is equivalent to ignoring inertia and leads to the equation of motion contain only a first time derivative. Absorbing a coefficient of proportionality into the time scale, we thus arrive at the *time-dependent Ginsburg-Landau (TDGL) equation*

$$\frac{\partial m}{\partial t}=-\frac{\delta F}{\delta m}=\nabla^2 m-V'(m). \tag{7.2}$$

  The TDGL equation is one of the central equations of coarsening, in spite of the fact that a gradient dynamics is impossible to derive from a microscopic theory, such as the Ising-Glauber model.

There are two important aspects of the TDGL equation that we would like to emphasize. First the TDGL equation is purely dissipative. Mathematically, this feature follows immediately by computing the change in the free energy as a function of time: following computation:

$$\frac{dF}{dt}=\int d\mathbf{x}\,\frac{\delta F}{\delta m}\,\frac{\partial m}{\partial t}=-\int d\mathbf{x}\,\left(\frac{\delta F}{\delta m}\right)^2\leq 0.$$

Thus a system governed by the TDGL equation simply "flows" down the free energy gradient until one of the minima of the potential is reached.

A second interesting point is that the TDGL equation has a natural interpretation as a reaction-diffusion process. For the standard potential $V(m)=\frac{1}{2}\,(1-m^2)^2$, the TDGL equation is, explicitly:

$$\frac{\partial m}{\partial t}=\nabla^2 m+2m(1-m^2). \tag{7.3}$$

If we view m as a density, then Eq. (7.4) describes the evolution of a diffusing population of m particles that react via birth, $m\to 2m$, and 3-body coalescence, $3m\to m$. The rate equation for this reaction, $\dot{m}=2m-2m^3$ has an unstable fixed point at $m=0$ and a stable fixed point at $m=1$. When diffusion is included, the resulting master equation (7.4) describes the infiltration of a stable high-density phase ($m=1$) into a low-density ($m=0$) region. In fact, Eq. (7.4) is just one example of the family of self-regulating reactions of the form

$$\frac{\partial m}{\partial t}=\nabla^2 m+f(m), \tag{7.4}$$

with $f(0)=f(1)=0$, $f(m)>0$ for $0<m<1$, and $f(m)$ having a single maximum in the range $[0,1]$. The most famous of this class of equations arises when $f(m)=m(1-m)$, and is known as the Fisher-Kolmogorov-Petrovsky-Piscounov (FKPP) equation (see the highlight below).

The FKPP Equation

The FKPP equation

$$\frac{\partial A}{\partial t} = D\nabla^2 A + kA(N-A), \tag{7.5}$$

describes the evolution of a population density A that diffuses and also reacts by birth ($A \to A + A$) and quadratic self-regulation ($A + A \to A$). If spatial fluctuations are neglected then in the resulting rate equation, $\dot{A} = A(N-A)$, there is a stable fixed point when $A = N$ and an unstable fixed point for $A = 0$. Here N should be viewed as the maximum number of particles that can be accommodated on a single site in the lattice version of the process. Starting with any non-zero density in a finite system, a final density of N is reached. A particularly relevant situation for population biology is the case where $A = N$ in the half-space $x < 0$ and $A = 0$ for $x > 0$. By diffusion alone, the sharp interface between these two regions would become more gentle. However, because of the interplay between diffusion and reaction, the stable high-density phase propagates as a stationary wave into the low-density phase. The nature of this wave propagation has been intensively investigated and many important features have been discovered.

Let's try to understand the basics of this wave propagation for a one-dimensional system. Proceeding in the most naive way possible, we assume that the infiltration of the stable state proceeds by a stationary propagating wave. As a preliminary, it is useful to rescale the density by $A \to A/N$, time by $t \to kt$, and then the length by $x \to x\sqrt{k/D}$ to non-dimensionalize the FKPP equation to $A_t = \nabla^2 A + A(1-A)$. The simplest assumption is that the leading edge of this wave decays exponentially with position. Thus we write

$$A(x,t) \sim e^{-\lambda(x-vt)}\,.$$

Substituting this form into Eq. (7.5) and dropping the non-linear term that is negligible at the leading edge of the wave, we obtain the dispersion relation

$$v = \lambda + \frac{1}{\lambda}.$$

Thus the velocity depends on λ and we can only surmise that $v \geq 2$. The equation of motion does not provide any further information about which value of λ should be selected. However, Nature appears to be wise and typically "selects" the minimum velocity $v_{\min} = 2$ that arises when $\lambda = 1$. In fact, for most "reasonable" initial conditions, this minimum velocity is the one that is actually selected.

More precisely, if the initial density decays as $e^{-\lambda_0 x}$ with $\lambda_0 < 1$, then the leading edge of the wave asymptotically evolves to an exponential with decay parameter $\lambda = 1$ and velocity $v = v_{\min}$. We call such wavefronts "sharp". On the other hand, if $\lambda_0 > 1$, then the leading edge of the wave preserves this slower decay, $e^{-\lambda_0(x-vt)}$, and the velocity is $v = \lambda_0 + \lambda_0^{-1} > v_{\min}$. However, this behavior is still not the full story! A full analysis for the FKPP equation shows that for an initially sharp wavefront the velocity slowly approaches its asymptotic value as $v(t) = v_{\min}(1 - 3/Nt)$. Moreover, in the leading edge of the wave, the density is small and there is no reason that the evolution of the first few invaders can even be described by a continuum equation. If one accounts for the discrete nature of the particles, then the wave velocity is reduced compared to the continuum value: $v = v_{\min}(1 - \pi^2/\ln^2 N)$—surprisingly rich behavior from a basic and paradigmatic equation of motion.

Conservative dynamics

In alloy systems, the natural order parameter is the difference in the concentration of the two constituent elements. By its construction, this order parameter is conserved in an isolated lump of alloy. Thus a different type of dynamics is needed to account for this microscopic conservation of material. Again, at a phenomenological level, we seek a governing dynamical equation that ensures that the flux of atoms of each element of the alloy can be expressed in the form of a (conserved) continuity equation

$$\frac{\partial m}{\partial t} + \nabla \cdot \mathbf{J} = 0, \tag{7.6}$$

where we again consider overdamped dynamics so that the equation of motion is first order in time. In Eq. (7.50), the flux vector $\mathbf{J}$ should depend on the order parameter through the free energy (7.1). The simplest choice that is both conservative and involves simple gradient flow is $\mathbf{J} \propto -\nabla \frac{\delta F}{\delta m}$. We again absorb the proportionality factor into the time scale to then obtain the equation of motion

$$\frac{\partial m}{\partial t} = \nabla^2 \frac{\delta F}{\delta m} = -\nabla^2 \left[\nabla^2 m - V'(m)\right]. \tag{7.7}$$

This is the *Cahn-Hilliard (CH) equation* for zero-temperature conservative dynamics.

The absence of thermal noise in Eqs. (7.2) & (7.7) suggests that we are effectively dealing with systems at zero temperature. To phenomenologically model the behavior at a positive temperature, we should add a (Langevin) noise term to the right-hand side of (7.2) or (7.7). There is a belief that this additional term should not change qualitative dynamical behavior as long as the temperature is below the critical temperature T_c. This belief boils down to the hypothesis that under renormalization, there are three possible behaviors:

- zero-temperature dynamics in which dynamical behavior is essentially the same for all $T < T_c$;
- critical dynamics ($T = T_c$);
- infinite-temperature dynamics in which the dynamical behavior for all $T > T_c$ are essentially the same, and trivial.

In this chapter, we will primarily discuss zero-temperature dynamics because this case embodies many of the outstanding issues associated with coarsening.

Typically, one starts with the initial temperature $T_i = \infty$ where the system is completely disordered and quenches the system to $T_f = 0$. The coarse-grained form of this disordered initial condition is

$$\langle m(\mathbf{x}, 0)\rangle = 0, \quad \langle m(\mathbf{x}, 0)\, m(\mathbf{x}', 0)\rangle = \delta(\mathbf{x} - \mathbf{x}'). \tag{7.8}$$

Thus the mathematical challenge is to determine the long-time behavior of the solutions of the *deterministic* nonlinear partial differential equations (7.2) and (7.7) subject to the *random* initial conditions (7.8).

7.2 Free Evolution

Numerical and analytical work has clearly shown that the solutions of (7.2) and (7.7) exhibit scaling, *i.e.*, a scale-invariant morphology of a coarsening domain mosaic develops at late times. This morphology is (statistically) independent of time when all lengths are rescaled by the typical domain size $L(t)$. This length scale grows algebraically with time, $L(t) \sim t^z$, with a nearly universal dynamical exponent z:

$$z = \begin{cases} 1/2 & \text{(TDGL);} \\ 1/3 & \text{(CH);} \end{cases} \tag{7.9}$$

for systems with a scalar order parameter. One important exception to the prediction of Eq. (7.9) is one dimension, where we shall derive that domains grow logarithmically in time for the TDGL equation, $L(t) \sim \ln t$, so that the dynamical exponent $z = 0$.

As always, scaling greatly simplifies the description of the dynamics. The evidence in favor of scaling is compelling, but it has not been proven except for the TDGL in one dimension and for a small class of microscopic models, such as the one-dimensional Ising-Glauber model and the n-vector model with $n = \infty$. It is therefore important to show that scaling arises in the TDGL and the CH equations, even for an oversimplified setting. Such an example is provided by the toy model where the potential vanishes, $V(m) = 0$. The dynamical equation then reduces to the diffusion equation, $m_t = \nabla^2 m$, for a non-conserved order parameter, and to the bidiffusion equation, $m_t = -\nabla^4 m$, for a conserved order parameter. In these cases, the presence of a single growing length scale, $L(t) \sim t^{1/2}$ (TDGL), and $L(t) \sim t^{1/4}$ (CH), is obvious from dimensional analysis (see the subsections on dimensional analysis and scaling in Sec. 1.1 for further discussion of this point).

If a spin system is initially in the random state specified by Eq. (7.8), then the mean magnetization remains zero throughout the evolution. We therefore need to study two-body correlation functions to probe the nature of the coarsening; we already encountered this same issue in our study of the voter model and the Ising-Glauber model in the previous chapter. We thus define the two-body correlation function

$$C(\mathbf{r}_1, t_1, \mathbf{r}_2, t_2) \equiv= \frac{\langle m(\mathbf{r}_1, t_1)\, m(\mathbf{r}_2, t_2)\rangle}{\sqrt{\langle m^2(\mathbf{r}_1, t_1)\rangle\, \langle m^2(\mathbf{r}_2, t_2)\rangle}} \tag{7.10}$$

to probe the domain structure at two different space-time points. The normalization is convenient because it makes the correlation function dimensionless. For simplicity, we use the shorthand $1 \equiv (\mathbf{x}_1, t_1)$ and $2 \equiv (\mathbf{x}_2, t_2)$. Translational invariance implies that $C(1,2) = C(\mathbf{r}, t_1, t_2)$ with $\mathbf{r} = \mathbf{r}_1 - \mathbf{r}_2$. It is also useful to explicitly study the *autocorrelation function* $A(t_1, t_2) = C(\mathbf{0}, t_1, t_2)$ which measures the probability that the sign of the magnetization coincides at times t_1 and t_2.

Let's begin by investigating coarsening in the the potential-free TDLG (diffusion) equation

$$\frac{\partial m}{\partial t} = \nabla^2 m \tag{7.11}$$

for the random initial condition of Eq. (7.8). The solution is

$$m(\mathbf{r}_1, t) = \frac{1}{(4\pi t)^{d/2}} \int m(\mathbf{r}_1, 0) e^{-(\mathbf{r}_1 - \mathbf{z}_1)^2/4t}\, d\mathbf{z}_1.$$

Then the average of the product of the magnetization at two different space-time points is

$$\begin{aligned}
\langle m(\mathbf{r}_1, t_1) m(\mathbf{r}_2, t_2)\rangle &= \frac{1}{[(4\pi)^2 t_1 t_2]^{d/2}} \iint \underbrace{\langle m(\mathbf{r}_1, 0)\, m(\mathbf{r}_2, 0)\rangle}_{\delta(\mathbf{r}_1 - \mathbf{r}_2)} e^{-(\mathbf{r}_1 - \mathbf{z}_1)^2/4t}\, e^{-(\mathbf{r}_2 - \mathbf{z}_2)^2/4t}\; d\mathbf{z}_1 d\mathbf{z}_2 \\
&= \frac{1}{[(4\pi)^2 t_1 t_2]^{d/2}} \int e^{-(\mathbf{r}_1 - \mathbf{z})^2/4t_1}\, e^{-(\mathbf{r}_2 - \mathbf{z})^2/4t_2}\; d\mathbf{z} \\
&= \frac{1}{[(4\pi)^2 t_1 t_2]^{d/2}} \int e^{-\mathbf{r}_1^2/4t_1}\, e^{-\mathbf{r}_2^2/4t_2}\, e^{-z^2(1/4t_1 + 1/4t_2)}\, e^{\mathbf{z}\cdot(\mathbf{r}_1/2t_1 + \mathbf{r}_2/2t_2)}.
\end{aligned}$$

We now perform the integral in the last line by completing the square in the exponential to give

$$\langle m(\mathbf{r}_1, t_1) m(\mathbf{r}_2, t_2)\rangle = \frac{1}{[4\pi(t_1 + t_2)]^{d/2}}\, e^{-(\mathbf{r}_1 - \mathbf{r}_2)^2/4(t_1 + t_2)}. \tag{7.12}$$

Finally, the normalized two-body correlation function defined by Eq. (7.10) is

$$C(1,2) = \left[\frac{2\sqrt{t_1 t_2}}{t_1 + t_2}\right]^{d/4} e^{-(\mathbf{r}_1 - \mathbf{r}_2)^2/4(t_1 + t_2)}. \tag{7.13}$$

Let's now perform the corresponding calculation for the potential-free CH (bidiffusion) equation

$$\frac{\partial m}{\partial t} = -\nabla^4 m, . \tag{7.14}$$

Both in this case and also for the diffusion equation, it is simplest to apply Fourier transform methods. Using the Fourier expansion $m(\mathbf{r}, t) = (2\pi)^{-d} \int d\mathbf{k}\, \hat{m}(\mathbf{k}, t)\, e^{-i\mathbf{k}\cdot\mathbf{r}}$ reduces (7.14) to an algebraic equation whose solution is simply $\hat{m}(\mathbf{k}, t) = \hat{m}_0(\mathbf{k})\, e^{-k^4 t}$, with $\hat{m}_0(\mathbf{k}) \equiv \hat{m}(\mathbf{k}, t = 0)$. Inverting this Fourier transform gives

$$m(\mathbf{x}, t) = (2\pi)^{-d} \int \hat{m}_0(\mathbf{k})\, e^{-i\mathbf{k}\cdot\mathbf{x} - k^4 t}\, d\mathbf{k}. \tag{7.15}$$

For the white noise initial condition, the initial value of the correlation function in Fourier space is just

$$\langle \hat{m}_0(\mathbf{k})\rangle = 0, \quad \langle \hat{m}_0(\mathbf{k})\, \hat{m}_0(\mathbf{k}')\rangle = (2\pi)^d \delta(\mathbf{k} + \mathbf{k}'). \tag{7.16}$$

Using these facts, the mean-square magentization $\langle m^2(\mathbf{x}, t)\rangle$ can be immediately found from Eqs. (7.15), (7.8) & (7.16), and the result is:

$$\langle m^2(\mathbf{x}, t)\rangle = (2\pi)^{-d} \int e^{-2k^4 t} = B_d (2t)^{-d/4}\, d\mathbf{k}, \tag{7.17}$$

with $B_d = (2\pi)^{-d}\Omega_d\Gamma(d/4)/4$, where $\Omega_d = 2\pi^{d/2}/\Gamma(d/2)$ is the area of the unit sphere in d dimensions, Γ the Euler gamma function, and the subscript d refers to the spatial dimension of the system.

Similarly, the correlation function is

$$\langle m(1)\, m(2)\rangle = (2\pi)^{-d}\int d\mathbf{k}\, e^{-i\mathbf{k}\cdot\mathbf{r}-k^4(t_1+t_2)}. \tag{7.18}$$

When spatial points coincide, $\mathbf{r}=\mathbf{0}$, we obtain the autocorrelation function

$$A(t_1,t_2) = \left[\frac{2\sqrt{t_1 t_2}}{t_1+t_2}\right]^{d/4}, \tag{7.19}$$

which has the same form for both the diffusion (see Eq. eqrefc8:2body-diff) and the bidiffusion equation. If the spatial points are different, $\mathbf{r}_1 \neq \mathbf{r}_2$, we perform the integral in Eq. (7.18) by introducing (for $d \geq 2$) spherical coordinates in $\mathbf{k}$-space so that $\mathbf{k}\cdot\mathbf{r} = kr\cos\theta$ and $d\mathbf{k} = k^{d-1}dk\,\Omega_{d-1}\sin^{d-2}\theta\, d\theta$ to give

$$\langle m(1)\, m(2)\rangle = \frac{\Omega_{d-1}}{(2\pi)^d}\int_0^\infty dk\, k^{d-1}\, e^{-k^4(t_1+t_2)}\, F_d(kr),$$

where

$$F_d(u) = \int_0^\pi d\theta\, (\sin\theta)^{d-2}\, e^{-iu\cos\theta}.$$

This integral may be readily determined for $d \leq 3$ and the two-body correlation function $C_d(r,t_1,t_2)$ is given by

$$C_d(r,t_1,t_2) = \begin{cases} \dfrac{2(4t_1t_2)^{1/8}}{\Gamma(1/4)\, r}\displaystyle\int_{-\infty}^\infty dq\, \cos q\, e^{-q^4\tau} & d=1; \\[2ex] \dfrac{4(4t_1t_2)^{1/4}}{\sqrt{\pi}\, r^2}\displaystyle\int_0^\infty dq\, q\, I_0(q)\, e^{-q^4\tau} & d=2; \\[2ex] \dfrac{2(4t_1t_2)^{3/8}}{\Gamma(3/4)\, r^3}\displaystyle\int_0^\infty dq\, q\, \sin q\, e^{-q^4\tau} & d=3. \end{cases} \tag{7.20}$$

In these equations, we used shorthand notations $q = kr$, $\tau = (t_1+t_2)/r^4$, and I_0 is the modified Bessel function of order 0.

Finally, the *temporally normalized* correlation function $G(\mathbf{r},t_1,t_2) \equiv C(\mathbf{r},t_1,t_2)/A(t_1,t_2)$ is a function of a *single* scaling variable τ (here the term "temporally normalized" reflects the property $G(\mathbf{0},t_1,t_2) \equiv 1$). This single-parameter scaling is a peculiarity of the toy model rather than a universal rule; generally, rotational symmetry and dynamical scaling would imply that $G(\mathbf{r},t_1,t_2)$ is a function of two variables. Finally at equal times $t_1 = t_2 = t$, both correlation functions $C_d(\mathbf{r},t,t)$ and $G_d(\mathbf{r},t,t)$ reduce to the equal-time correlation function $G_d(\tau)$ which is the function of the single scaling variable $\tau = 2t/r^4$. For the potential-free CH equation, the precise form of the equal-time correlation function $G_d(\tau)$ is

$$G_d(\tau) = \begin{cases} \dfrac{2\tau^{1/4}}{\Gamma(1/4)}\displaystyle\int_{-\infty}^\infty dq\, \cos q\, e^{-q^4\tau} & d=1; \\[2ex] \dfrac{4\tau^{1/2}}{\sqrt{\pi}}\displaystyle\int_0^\infty dq\, q\, I_0(q)\, e^{-q^4\tau} & d=2; \\[2ex] \dfrac{2\tau^{3/4}}{\Gamma(3/4)}\displaystyle\int_0^\infty dq\, q\, \sin q\, e^{-q^4\tau} & d=3. \end{cases}$$

7.3 Case Studies in Non-Conservative Dynamics

We now leave the investigation of generalities and discuss explicit solutions of the basic equations of motion. Because the geometry of the interfaces between domains is generally quite complex, we seek the simplest possible settings where the geometry is sufficiently simple to admit an exact analysis yet still allows for non-trivial dynamics. There are several such systems, such as the classic examples of a single domain wall and a single spherical droplet. We also discuss several other examples that are not so widely appreciated yet are rich laboratories to develop our understanding. These include a single finger, a single wedge, and an isolated shrinking grain.

Straight domain wall

The simplest example of an interface is, of course, a flat domain wall. For the discrete Ising-Glauber model, a flat interface is trivial because the spin merely changes sign across a particular hyperplane. For the continuum TDGL equation, a flat interface is a bit more interesting because there is a non-trivial spatial variation of the coarse-grained magnetization across the domain wall. Since a flat interface is stationary, the order parameter satisfies the ordinary differential equation

$$\frac{d^2m}{dx^2} = V'(m), \tag{7.21}$$

subject to the boundary conditions $m(\pm\infty) = \pm 1$ that lead to the domain wall being stationary.

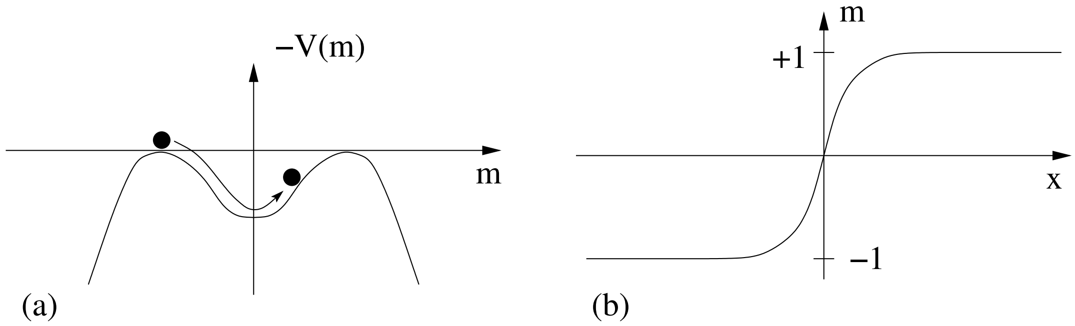

Figure 7.1: (a) The effective potential $-V(x) = -\frac{1}{2}(1-m^2)^2$ and the motion of the analogue particle that corresponds to a single kink. The particle starts at the top of the left maximum at $m = -1$ and moves without dissipation until it eventually stops at the maximum at $m = +1$. (b) The corresponding dependence of m on x.

Before solving (7.21), we emphasize a neat interpretation of the domain wall in terms of classical mechanics: Treating x as the time variable and m as the coordinate, we see that the problem is equivalent to the motion of a fictitious, analogue particle of mass one in the potential $-V$. The energy of this analogue particle

$$E = \frac{1}{2}\left(\frac{dm}{dx}\right)^2 - V(m) \tag{7.22}$$

does not change with "time" x. The boundary conditions imply that the total energy equals zero. Thus $\frac{dm}{dx} = \sqrt{2V(m)}$, or

$$x = \int_{m(0)}^{m(x)} \frac{d\mu}{\sqrt{2V(\mu)}}\,, \tag{7.23}$$

where it is customary to set $m(x=0) = 0$. For the classic potential $V(m) = \frac{1}{2}\,(1-m^2)^2$, the domain wall profile is then

$$m(x) = \tanh x\,. \tag{7.24}$$

This solution is known as a "kink" in a ϕ^4 theory. The width of the kink in this example is of the order of one. The free energy density of the kink is

$$\frac{1}{2}\left(\frac{dm}{dx}\right)^2 + V(m) = 2V(m(x)) = \frac{1}{\cosh^4 x}, \tag{7.25}$$

and the total free energy per unit area, that is, the surface tension, is

$$\sigma = \int_{-\infty}^{\infty} 2V(m)\, dx = \int_{-\infty}^{\infty} 2V(m)\left(\frac{dm}{dx}\right)^{-1} dm = \int_{-1}^{1} \sqrt{2V(m)}\, dm = \frac{4}{3}\,. \tag{7.26}$$

Within the classical mechanical analogy, the governing equation (7.21) can of course be derived by minimizing the "action"

$$\int_{-\infty}^{\infty} dx \left[\frac{1}{2}\left(\frac{dm}{dx}\right)^2 + V(m)\right],$$

so that the action associated with the analogue particle coincides with the surface tension.

The mechanical analogy provides many useful insights about the phase behavior of a system even in situations where an analytical description of the domain walls is not feasible. For example, imagine that there is an initial condition that has the form of a combination of two static solutions, such as a kink-antikink configuration. That is, the order parameter starts at $m \approx -1$ for $x \to \infty$, then increases to $m \approx +1$ over an intermediate range of x, and then returns to the value $m \approx -1$ for $x \to +\infty$. Can such a configuration be stable? Within the mechanical analogue, we are asking if it is possible for the analogue particle to start at the maximum at $m = -1$, move to the maximum at $m = +1$, and then return to the maximum at $m = -1$ (see Fig. 7.1). Clearly this type of motion is impossible, so we conclude without calculation that a kink-antikink pair cannot be stable. Numerical simulations show that the kink and antikink slowly move toward each other and eventually annihilate. We shall analyze this motion later in this chapter.

Another useful aspect of the mechanical analogy is that it can characterize *all* possible one-dimensional stationary solutions that correspond to a finite free energy per unit area. For any potential function, the analogue particle (i) must start at one maximum of the potential $[-V]$ at $x = -\infty$ and reach another maximum of the potential $[-V]$ at $x = \infty$, and (ii) if the maxima are different, they must be adjacent. Thus for potentials with two degenerate minima (at $m = \pm 1$) there are two types of static solutions—a kink and an antikink—that we symbolically denote as $[-1, 1]$ and $[1, -1]$, respectively. Similarly for potentials with three three degenerate minima (for example, a 3-state spin system with minima at $m = \pm 1$ and $m = 0$) there are four types of static solutions: $[-1, 0], [0, -1], [1, 0], [0, 1]$. A domain wall of the form $[-1, 1]$ cannot occur. To be concrete, for the potential $V(m) = \frac{1}{2}\, m^2\,(1 - m^2)^2$, the exact static solutions of Eq. (7.23) that separate the phases with $m = 0$ and $m = \pm 1$ are

$$m(x) = \pm\left(1 + e^{\pm x}\right)^{-1/2}\,. \tag{7.27}$$

Higher dimensions

Let's now investigate higher dimensions. Perhaps the simplest situation is the evolution of a small droplet of one phase with $m = -1$ in a sea of the opposite phase with $m = 1$. From the perspective of the individual spins, we expect that a small cluster of minority spins will be overwhelmed by the large majority of oppositely-oriented spins. This is precisely what happens in the continuum picture. The consideration of a small droplet avoids all the complexities associated with the tortuous interface between two competing phases, as the droplet becomes spherical as it shrinks to zero at long times.

Since the droplet shrinks, we must use the full time-dependent TDGL equation to describe its evolution. The TDGL equation (7.2) simplifies due to spherical symmetry:

$$\frac{\partial m}{\partial t} = \frac{\partial^2 m}{\partial r^2} + \frac{d-1}{r}\frac{\partial m}{\partial r} - V'(m). \tag{7.28}$$

Provided that the droplet radius R greatly exceeds the interface width, we anticipate that solution has the form

$$m(r,t) = f(x), \qquad x = r - R(t). \tag{7.29}$$

Substituting this ansatz into (7.28) gives

$$f'' + \left(\frac{d-1}{r} + \frac{dR}{dt}\right) f' - V'(f) = 0. \tag{7.30}$$

Let's now multiply this equation by f' and integrate with respect to x through the interface. Since the interface is sharp and localized near $R(t)$ that grows with time, we can set the lower limits of the integrals, $x = -R$, to $-\infty$. This gives

$$(f')^2\Big|_{-\infty}^{\infty} + \int_{-\infty}^{\infty} \left(\frac{d-1}{r} + \frac{dR}{dt}\right)(f')^2\, dx - V(x)\Big|_{-\infty}^{\infty} = 0. \tag{7.31}$$

We now use the fact that $f(x)$ changes suddenly from -1 to 1 near $x = 0$ (corresponding to $r = R(t)$), so that f' is sharply peaked near the origin. Thus the first term vanishes. Similarly, the last term is zero, since the potential has the same value at $x = \pm\infty$. Finally, the integral is non-zero only very close to $x = 0$. Therefore

$$\frac{d-1}{R} + \frac{dR}{dt} = 0. \tag{7.32}$$

Solving this equation gives $R^2 = R_0^2 - 2(d-1)t$, so that the droplet shrinks to zero in a finite time $t \propto R_0^2$.

The virtue of this focus on the region near the interface is that instead of the unsolvable TDGL equation (7.28) we obtain a more tractable equation for the interface dynamics. Remarkably, this simplified description in terms of interface dynamics is possible for an arbitrarily complex domain geometry, provided that the characteristic length scale associated with the interface greatly exceeds its width. This construction is particularly simple in two dimensions. Locally an interface has a given curvature $1/R$ and therefore the interface can be approximated by a circle of radius R. Consequently, the velocity of shrinking normal to the interface is $v \approx -1/R$. Generally in d dimensions, the interface is a $(d-1)$-dimensional manifold and we denote by $R_1, \ldots, R_{d-1}$ its principal radii of curvature (which of course depend on the local position on the interface). Then the normal velocity of the interface is the sum of the principal curvatures $1/R_j$. The average of the curvatures is known as the *mean curvature*, $K = (d-1)^{-1}\sum 1/R_j$. Thus we arrive at the so-called Allen-Cahn equation for the normal velocity:

$$v = -(d-1)K. \tag{7.33}$$

There are two noteworthy points to make about the Allen-Cahn equation. First, it clearly does not apply in one dimension, where the interface between two domains is just a point. In this case, we shall see that the interface velocity is an exponentially small function of the domain lengths on either side of the interface. This feature leads to domains that grow logarithmically in time and to extremal dynamics in which only the smallest domain merges with its neighbors in an update event. A second point is that the interface dynamics derived from the TDGL equation is a specific example of curvature-driven flow where one is concerned with the evolution of general shapes in arbitrary dimension due to a local velocity that is proportional to the local curvature. Curvature-driven flows have been thoroughly investigated and much is known about evolution of a single closed interface. In two dimensions, every such interface asymptotically approaches a (shrinking) circular shape. The same happens in three dimensions if the initial interface is everywhere *convex*. However, an interface that contains both convex and concave portions can undergo fission if the concave portion of the manifold is sufficiently thin (think of the fission of a very elongated liquid drop in which the neck of fluid in the middle is extremeley thin. The classification of all possible topology changes in higher dimensions due to curvature-driven flow is still incomplete.

Two-dimensional unbounded domains

A beautiful set of domain evolution problems is inspired by returning to a discrete Ising spin system on the square lattice and asking: what are the simplest initial states for which evolution under zero-temperature Glauber dynamics can be studied analytically? The first example of this type is a single straight domain wall that cuts a finite system in two. This example is too simple, however, as a straight domain is static under zero-temperature Glauber dynamics. To have a system that actually evolves, the initial interface must contain at least one corner. In this section, we investigate two examples of this type (Fig. 7.2):

- the semi-infinite finger (2 initial corners);
- the 90° infinite wedge (1 initial corner).

Curiously, although the finger appears to be more complex than the wedge because there are two initial corners, its dynamics is simpler than that of the wedge. The wedge is, in fact, extremely rich, with nice connections between the shape of the wedge and the famous number theoretic problem of the partitioning of the integers.

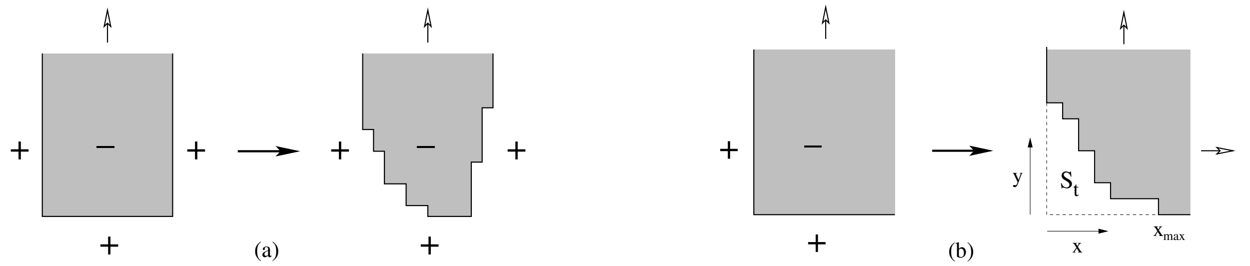

Figure 7.2: (a) A semi-infinite finger and (b) a 90° infinite wedge, showing both the initial state (left of each figure) and the system at a later time (right side). The spin down region is shown shaded. For the wedge, the evolving interface encloses an area S_t at time t.

Let's begin with the semi-infinite finger. At the microscopic level of individual spins, the interface will develop a series of terraces that culminate at the tip. At the tip there can even be pinch off of islands when the finger has shrunk laterally to a unit width. A detailed understanding of these microscopic details has yet to be achieved. However, within the continuum description the asymptotic behavior is quite simple. Let the minority phase initially occupy the semi-infinite region $y > 0$ and $|x| < L$. The interesting limit is $t \gg L^2$ where sufficient time has elapsed so that the two corners of the initial finger interact. In this long-time regime, the finger relaxes to a limiting shape that recedes at a constant velocity. In a reference frame that moves with the finger, the interface $y(x)$ is thus stationary.

For this geometry, the Allen-Cahn equation is

$$v_n = \frac{y''}{[1 + (y')^2]^{3/2}}. \tag{7.34}$$

Here v_n is the velocity normal to the interface and the right-hand side is just the curvature associated with the locus $y(x)$ that defines the boundary of the finger and the prime denotes differentiation with respect to x. In the steady state, only the vertical component of the velocity is relevant. From Fig. 7.3, the vertical velocity v_y is given by $v_y = v_n/\cos\theta = v_n\sqrt{1 + (y')^2}$. Thus the equation satisfied by the vertical velocity is simply

$$v_y = \frac{y''}{1 + (y')^2} \tag{7.35}$$

subject to the boundary condition $y \to \infty$ when $|x| \to L$. This equation can be integrated by elementary methods and the result is

$$y = -\frac{2L}{\pi} \ln\left[\cos\left(\frac{\pi x}{2L}\right)\right]. \tag{7.36}$$

In this steady state, the finger recedes at a constant velocity $v = \pi/2L$.

Next let's study an infinite wedge domain (Fig. 7.2). For concreteness, we define the initial corner to be at the origin so that the wedge initially occupies the region $x, y \geq 0$. The corner of the wedge recedes diffusively $x, y \propto \sqrt{t}$ both in the framework of the Ising-Glauber dynamics and in the continuum description. Because of the absence of any constant with dimension of length in Eq. (7.35), the corresponding solution admits the self-similar form

$$X = x(t)/\sqrt{t}, \qquad Y(X) = y(x,t)/\sqrt{t}\,, \quad . \tag{7.37}$$

Notice that the increase of the magnetization is equal to twice the area under the curve $y(x,t)$. Using (7.37), the growth of the area is proportional to t, so that the magnetization also grows linearly with time. To

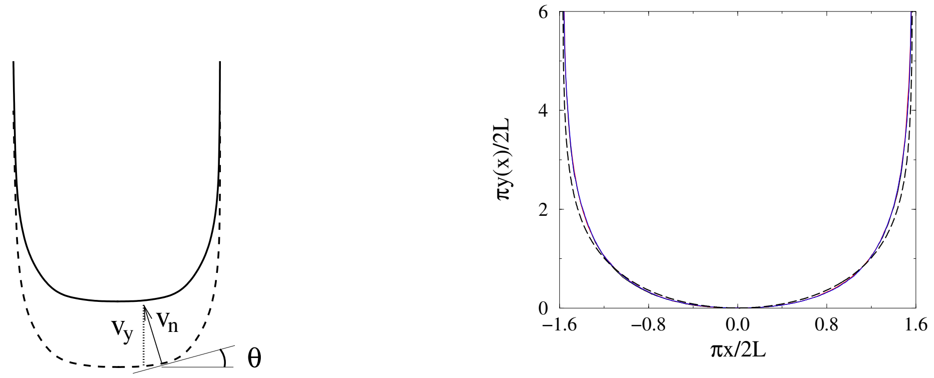

Figure 7.3: (Left) Schematic illustration of the receding finger showing the relation between the normal velocity v_n and the vertical velocity v_y. (Right) Comparison of the finger shape predicted by the TDGL approach given in Eq. 7.36 (dashed line) with simulation results for 100 realizations of width $2L = 400$ at times $t = 2 \times 10^5$, 6×10^5, and 10^6 steps (solid lines). The data for these three times essentially coincide.

determine the evolution of the wedge shape, we substitute the ansatz Eq. (7.37) into the equation of motion (7.35) and find that the scaling function $Y(X)$ obeys

$$\frac{Y - XY'}{2} = \frac{Y''}{1 + (Y')^2}, \tag{7.38}$$

where prime indicates differentiation with respect to X. Equation (7.38) should be solved subject to the constraints

$$\lim_{X\to\infty} Y(X) = 0, \qquad \lim_{X\to+0} Y(X) = \infty. \tag{7.39}$$

Within the continuum framework, one could also study the evolution of a wedge with an arbitrary opening angle. If the wedge initially occupies the region $y > |x| \tan\theta$ we should solve Eq. (7.38) subject to the boundary condition $Y \to \pm X \tan\theta$ as $X \to \pm\infty$.

To solve Eq. (7.38), we introduce the polar coordinates $(X, Y) = (r\cos\theta, r\sin\theta)$ to recast it into the following equation for $r = r(\theta)$, after straightforward variable transformations:

$$2r\,\frac{d^2r}{d\theta^2} - \left(4 + r^2\right)\left(\frac{dr}{d\theta}\right)^2 = r^2\left(2 + r^2\right). \tag{7.40}$$

Writing $\frac{dr}{d\theta} = R(r)$, reduces Eq. (7.40) to a first-order equation whose solution is $R^2 = r^4\, e^{r^2/2}\, F(r, r_*)$, with

$$F(r, r_*) = \int_{r_*}^{r} d\rho\, \left(\frac{2}{\rho^3} + \frac{1}{\rho}\right) e^{-\rho^2/2}\,, \tag{7.41}$$

and r_* is the scaled distance from the origin to the closest point on the interface. The interface is now determined from

$$\frac{dr}{d\theta} = \pm r^2\, e^{r^2/4} \sqrt{F(r, r_*)}, \tag{7.42}$$

with the plus sign for $\theta \geq \pi/4$ and the minus sign for $\theta \leq \pi/4$ to give a symmetric solution about the diagonal $\theta < \pi/4$. Integrating Eq. (7.42) gives the explicit equation for $\theta = \theta(r)$

$$\theta = \int_r^\infty d\rho\, \rho^{-2}\, e^{-\rho^2/4}\, [F(\rho, r_*)]^{-1/2} \tag{7.43}$$

for $\theta \leq \pi/4$. For $\pi/4 < \theta < \pi/2$, we simply use $r(\theta) = r(\frac{\pi}{2} - \theta)$ to ensure symmetry of the interface about the diagonal. The value of the unknown r_* may now be obtained by ensuring that $\theta = \pi/4$ when $r = r_*$. This gives the criterion

$$\int_{r_*}^\infty dr\, r^{-2}\, e^{-r^2/4} [F(r, r_*)]^{-1/2} = \frac{\pi}{4}\,, \tag{7.44}$$

whose numerical solution is $r_* \approx 1.0445$. Equation (7.43), with F given by (7.41), provides an explicit representation of $\theta(r)$ on the interface in terms of the (scaled) distance $r \in [r_*, \infty)$ from the origin.

In the asymptotic regime $r \to \infty$, the interface becomes much simpler. From Eqs. (7.41) and (7.43) we obtain $\theta \to A\,r^{-3}\,e^{-r^2/4}$ with $A = 2\,[F(\infty, r_*)]^{-1/2}$ which, in Cartesian coordinates, is

$$Y \to A\,X^{-2}\,e^{-X^2/4}\,. \tag{7.45}$$

Apart from the numerical factor A, the asymptotic behavior follows directly from Eq. (7.38) after dropping the subdominant terms.

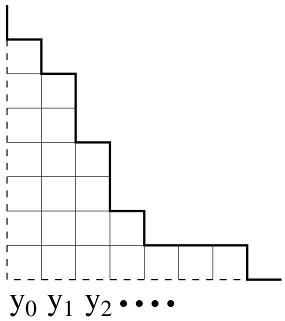

Figure 7.4: The Young diagram that is based on the interface profile of Fig. 7.2. This diagram corresponds to a partition of the integer 22 into the set $\{7, 6, 4, 2, 1, 1, 1\}$.

The staircase profile of the interface illustrated in Fig. 7.2(b) has a simple relation to the number-theoretic problem of the partitions of the integers. Given an arbitrary integer N, how many different ways can we break up this number into k integer pieces $n_1, n_2, \ldots, n_k$ with $\sum_k n_k = N$?. Geometrically, this question is the same as enumerating all possible interfaces with a given number of flipped spins in the wedge geometry! The interface height y_k and the k^{th} column is same as n_k in the partitioning problem. For $N \to \infty$, the staircase generated by its partition approaches a limiting shape. The equation for this shape is remarkably simple:

$$e^{-\lambda x} + e^{-\lambda y} = 1, \quad \text{with } \lambda = \frac{\pi}{6\sqrt{N}}. \tag{7.46}$$

In scaled units, the asymptotic shape of the integer partition limiting staircase is $Y \sim \frac{\sqrt{6}}{\pi} e^{-\pi X/\sqrt{6}}$, whereas the asymptotic Ising staircase is given by $Y \sim \frac{1.0445\ldots}{X^2}\,e^{-X^2/4}$. The existence of two distinct shapes arises from the different construction rules of the Ising interface and the interface generated by the integer partitions. In the partitioning of the integers, each staircase corresponding to fixed N is generated with the same weight. On the other hand, the Ising interface is generated dynamically and when its area reaches N, the interface contains an imprint of its entire history.

7.4 Conservative Dynamics

The phenomenon of coarsening in the case where the dynamics conserves the order parameter is a challenging theoretical problem. The existence of the conservation law severely limits the way in which an interface between two domains can move. While it is evident that an interface between two phases should move to reduce its local curvature and consequently the energy, such an evolution has to be accompanied by a global rearrangement of the interfaces so ensure that the order parameter is conserved. Dealing with this complexity led to the development of a range of theories, some of which were not consistent with each other.

On the other hand, much progress has been made in studying the coarsening dynamics in the simplest geometries, such as a single droplet or a dilute population of droplets immersed in a majority phase. Here, the geometry of each droplet remains spherical throughout the evolution so that one avoids the geometrical complexity associated with the coarsening of a random system. Although the kinetics of the droplet evolution in the dilute limit is both quite subtle and rich, it can be treated in a deductive way through the master equation approach. In this section, we will follow in this tradition of studying the dilute limit.

Evolution of a single droplet

As an essential preliminary, let's consider the how a single droplet of a one phase evolves when it is immersed in a background of the opposite phase. Already, we run into a basic problem. If the two phases were perfectly separated, then the droplet could not evolve because any change in the droplet size would violate the conservation of the order parameter. Instead, we should think of a single drop of liquid that is floating in a closed container of gas that is saturated with the liquid in vapor phase. At the surface of the liquid droplet there is both evaporation as well as condensation of vapor molecules back into the droplet. The condensation rate is given by the flux of vapor molecules to the droplet which, in turn, is determined by vapor concentration in the gas. In principle, the vapor concentration exterior to the droplet obeys the diffusion equation. However, we shall see that the droplet radius changes slowly with time; consequently, we ignore the time dependence and deal with the much simpler Laplace equation to determine the external vapor concentration. Effectively, we are applying the quasi-static approximation because the droplet radius changes sufficiently slowly that the vapor always remains close to its equilibrium density profile.

Schematically, the concentration of the minority phase as a function of distance from the center of a droplet of radius R should have the dependence sketch in Fig. 7.5. The average concentration of the

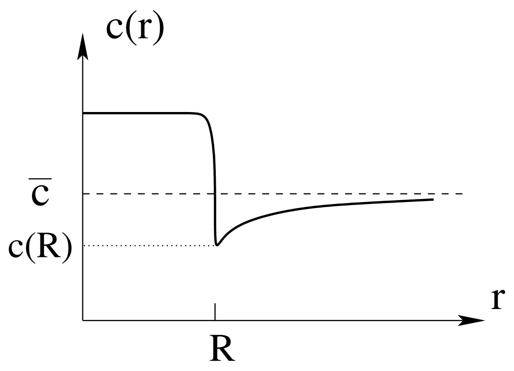

Figure 7.5: Dependence of the concentration of the minority phase as a function of radius.

minority phase in the entire system $\bar{c}$ must be larger than the supersaturation value c_∞, *i.e.*, there must be supersaturation, so that a droplet can form in the first place. Conversely, for $\bar{c} < c_\infty$, the minority phase remains as a homogeneous vapor in the gas. Inside the droplet, the concentration is much higher than $\bar{c}$ by the very definition of a droplet. Outside the droplet, the vapor concentration obeys Laplace's equation with the boundary conditions $c(r \to \infty) \to \bar{c}$ and $c(R)$ determined by the Gibbs-Thompson relation. In three dimensions, $c(r)$ thus is

$$c(r) = \bar{c} - [\bar{c} - c(R)]\,\frac{R}{r}. \tag{7.47}$$

The Gibbs-Thompson relation relates $c(R)$ to c_∞ by the following physical picture: For a bulk liquid in equilibrium with a saturated vapor, the concentration of vapor at the interface much be c_∞ by definition. For a small droplet, the vapor pressure is larger than that of a bulk liquid because a larger fraction of molecules are at the interface. Thus $c(R)$ should exceed c_∞ by an amount that vanishes as the droplet radius goes to infinity. This relationship is encapsulated by the Gibbs-Thompson relation $c(R) = c_\infty\left(1 + \frac{\nu}{R}\right)$, where ν is known as the capillary length and is simply related to the surface tension, c_∞, and the temperature.

Putting all these elements together, the rate of change of the volume V of an isolated droplet is given by

$$\frac{dV}{dt} = 4\pi R^2\,\frac{dR}{dt} = 4\pi R^2\, D\frac{\partial c}{\partial r}\Big|_{r=R}, \tag{7.48}$$

from which we obtain $\dot{R} = D[\bar{c} - c(R)]/R$. We now define $\Delta = \bar{c} - c_\infty$ as the degree of supersaturation and use the Gibbs-Thompson relation to eliminate $c(R)$ in (7.48) to give

$$\dot{R} = \frac{D}{R}\left(\Delta - \frac{\nu}{R}\right) \equiv \frac{\alpha}{R^2}\left(\frac{R}{R_c} - 1\right). \tag{7.49}$$

From the latter form of the above equation, it is clear that for $R > R_c = \Delta/\nu$ the droplet grows, while for $R < R_c$ the droplet shrinks. More importantly, this equation contains the seeds of $t^{1/3}$ coarsening. While an isolated supercritical droplet asymptotically grows as $t^{1/3}$, a subcritical droplet shrinks to zero size in a time that scales as the cube root of its initial radius. As we shall see in the next subsection, for a dilute population of droplets of differing sizes, the overall coarsening is governed by a $t^{1/3}$ growth law.

Lifshitz-Slyazov-Wagner coarsening

The discussion of the previous subsection provides the basis for understanding the coarsening of a dilute population of droplets of various sizes in a supersaturated background. This problem was independently analyzed by Lifshitz and Slyozov and by Wagner and we therefore refer to the problem as LSW coarsening. The dilute limit allows us to make the approximation that droplets are non-interacting. As a consequence the concentration field around each droplet is the same as that of an isolated droplet. The basic feature of this coarsening is already contained in Eq. (7.49): droplets whose radii is larger than R_c grow and those with smaller radii shrink. In a population of heterogeneous droplets, the value of R_c has to be determined self consistently, and we shall show that this calculation gives $R_c \propto t^{1/3}$.

Let $f(R,t)$, be the concentration of droplets of radius R at time t. This concentration evolves simply by the equation of continuity

$$\frac{\partial f}{\partial t} + \frac{\partial j}{\partial R} = 0, \tag{7.50}$$

where the flux $j = \dot{R} f(R,t)$ is just the difference between the inflow and outflow of droplets of radius R due to their evolution. We wish to solve this equation of motion with $\dot{R}$ given by Eq. (7.49) and subject to the constraint that the total mass of the minority phase is conserved. This gives

$$\bar{c} - c_\infty + \frac{4\pi}{3}\int_0^\infty R^3\, f(R,t)\, dR = \text{const.} \tag{7.51}$$

There is a subtle point with this conservation condition. In the minority limit the volume fraction of the minority phase that exists as freely diffusing monomers is vanishingly small. Thus the conservation law reduces to the total volume of the droplets is fixed. With this proviso, Eqs. (7.49), (7.50) and (7.51) constitute the governing equations of coarsening in the minority limit with a conserved order parameter.

To solve these equations of coarsening, it it again very useful to apply scaling. The natural scaling ansatz for this system, under the assumption that the mass of all droplets is conserved, is

$$f(R,t) = \frac{1}{R_c^4}\, \phi\left(\frac{R}{R_c}\right).$$

Here the prefactor is determined by the conservation of the total mass of the minority phase, namely, $\int R^3\, f(R,t)\, dR = \text{const.}$ Substituting this scaling ansatz into (7.50), the first term in this equation becomes

$$\frac{\partial f}{\partial t} = -\frac{\dot{R}_c}{R_c^5}\,\phi - \frac{1}{R_c^4}\,\phi'\,\frac{R\dot{R}_c}{R_c^2} = -\frac{\dot{R}_c}{R_c^5}(4\phi + z\phi'),$$

where the prime denotes differentiation with respect to the scaled variable $z \equiv R/R_c$. Similarly, the second term in (7.50) becomes

$$\frac{\partial}{\partial R}\left[\frac{\alpha}{R^2}\left(\frac{R}{R_c} - 1\right)\frac{1}{R_c^4}\,\phi\right] = \frac{\alpha}{R_c^7}\left[\left(\frac{1}{z} - \frac{1}{z^2}\right)\phi' + \left(\frac{2}{z^3} - \frac{1}{z^2}\right)\phi\right].$$

These preliminaries help convert the partial differential equation of (7.50) into the ordinary differential equation

$$R_c^2\dot{R}_c = \alpha\, \frac{\left[\left(\frac{1}{z} - \frac{1}{z^2}\right)\phi' + \left(\frac{2}{z^3} - \frac{1}{z^2}\right)\phi\right]}{4\phi + z\phi'} \equiv \alpha\gamma. \tag{7.52}$$

In writing the above equation, we rearranged the terms to put all the time dependence of the left side and all the z dependence on the right. Since both sides are functions of different variables they each must be constant. In many applications of scaling, the value of the separation constant plays little role in the scaling solution. In contrast, for coarsening, the separation constant γ plays an essential role. Depending on the value of γ, there are three different regimes of behavior, only one of which is physically meaningful.

Let us now examine the separated equations and thus determine the condition that gives the physical value of γ. For the time dependence we have

$$R_c^2\,\dot{R}_c = \alpha\gamma, \tag{7.53}$$

with solution

$$R_c(t) = (3\alpha\gamma t)^{1/3}. \tag{7.54}$$

Thus coarsening under the constraint of a conserved order parameter leads to a $t^{1/3}$ growth of the typical droplet radius. This slow growth of the typical droplet (compared to diffusive growth) provides the justification for the quasi-static approximation that was used to determine the concentration outside a droplet.

For the z dependence of the scaling function, the governing equation is, after some simple rearranging:

$$a\phi' + b\phi = 0, \qquad \text{with} \qquad a = -\frac{1}{z^2} + \frac{1}{z} - z\gamma, \quad b = \frac{2}{z^3} - \frac{1}{z^2} - 4\gamma. \tag{7.55}$$

Thus the scaling function is formally given by

$$\ln\phi = \int^z -\frac{b(y)}{a(y)}\,dy = \int^z \frac{2-y-4\gamma y^3}{1-y+\gamma y^3}\,\frac{dy}{y}. \tag{7.56}$$

Thus far, the reasoning is standard: we've used scaling to separate the partial differential equation (7.50) into two ordinary differential equations. As is generally the case, the time dependence then follows easily. For LSW coarsening, however, analysis of the z dependence is subtle, as the value of the separation constant γ is essential. The first basic and somewhat surprising fact from studying Eq. (7.56) is that $\phi(z)$ must have a sharp cutoff at a value $z_{\rm max}$, beyond which $\phi(z) = 0$. To demonstrate this fact, suppose the opposite is true. Then as $z \to \infty$, Eq. (7.56) would tell us that $\phi(z)$ should asymptotically vary as

$$\ln\phi \sim \int^z -4\,\frac{dy}{y} \sim -4\,\ln z \longrightarrow \phi \sim z^{-4}.$$

A power law tail for ϕ is impossible, however, as this asymptotic decay leads to a divergence of the total mass of the minority phase:

$$\int R^3\,\phi\,(R,t)\,dR \sim \int z^3\,z^{-4}\,dz \to \infty.$$

Thus we conclude that $\phi(z)$ has a sharp cutoff beyond some value $z_{\rm max}$.

A second and more profound fact is that only one value of the separation constant γ is physically allowed. To see why this is the case, let's re-examine the behavior of $\dot{R}$ in scaled units. Using both Eqs. (7.49) and (7.53), we find, after some simple algebra:

$$\dot{z} = \frac{1}{3\gamma t}\left(\frac{1}{z} - \frac{1}{z^2} - \gamma z\right) \equiv \frac{1}{3\gamma t}\,g(z). \tag{7.57}$$

Let's now examine the behavior of $g(z)$ for different values of γ. There are 3 cases:

(a) $\gamma < \gamma^* = 4/27$. Here $z(t)$ flows exponentially quickly to the stable fixed point at z_2 for $z(0) > z_1$ (see Fig. 7.6). That is, the radii of all droplets approach the common value $R_c z_2$, which diverges as $t \to \infty$. Such a distribution cannot satisfy mass conservation.

(b) $\gamma > \gamma*$. Here $z(t) \to 0$ exponentially quickly in time for any initial value of z. Thus all droplets shrink to zero and mass conservation is again violated.

(c) $\gamma = \gamma^*$. In this case $z = 3/2$ is a fixed point, but one that is approached as a power law in time. This subtle behavior is the mechanism that allows mass conservation to be satisfied. If the fixed point at $z = 3/2$ was reached exponentially quickly, then again all droplet radii would approach the common value of $3R_c/2$ and mass conservation would be violated. The slow decrease in z ensures the delicate balance between growth and shrinking of clusters in a mass-conserving way.

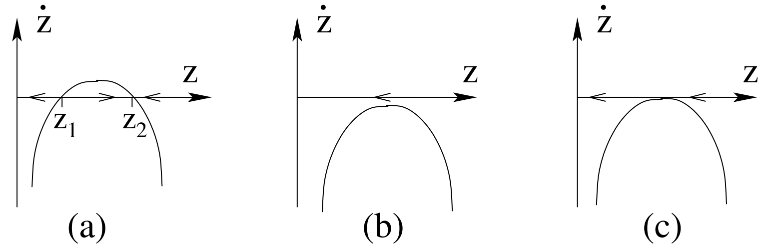

Figure 7.6: Sketch of $\dot{z} = g(z)/(3\gamma t)$ versus z for the 3 cases: (a) $\gamma < \gamma^*$, (b) $\gamma > \gamma^*$, and (c) $\gamma = \gamma^*$. The arrows on the $x = z$ axis shows the flow of z according to Eq. (7.57).

For the physical case of $\gamma = \gamma^*$, Eq. (7.56) for the scaling function can be factorized as

$$\ln \phi = \int^z \frac{2 - y - \frac{16}{27}y^3}{(y - \frac{3}{3})^2(y + 3)} \frac{dy}{y}.$$

Evaluating the latter integral by a partial fraction expansion now gives the remarkably rich form of the scaling function (for three dimensions):

$$\begin{aligned} \phi(z) &\propto z^2(z+3)^{-7/3}(3-2z)^{-11/3}\, e^{-3/(3-2z)} \quad && z < 3/2; \\ &= 0 && z > 3/2. \end{aligned} \tag{7.58}$$

A plot of this scaled droplet radius distribution is shown in Fig. 7.7

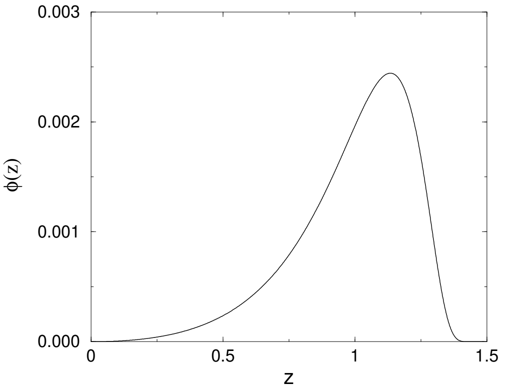

Figure 7.7: The scaling function $\phi(z)$ for LSW coarsening given by Eq. (7.58)

7.5 Extremal Dynamics

Shrinking of a single domain

While power-law domain growth is a generic feature of zero-temperature coarsening, there is one important case where much slower logarithmic growth occurs—the TDGL equation in one dimension. The case of one dimension is special because there is no local curvature to drive an interface; rather the interface moves by a net flux of order parameter across neighboring domains that, in turn, is determined by their lengths. We shall see that in the long-time limit, this flux vanishes as e^{-L}, where L is the length of a typical domain; the smallness of the flux is ultimately responsible for logarithmic coarsening. As a consequence of this slow growth, the asymptotic dynamics of the one-dimensional TDGL equation has an extremal character in which

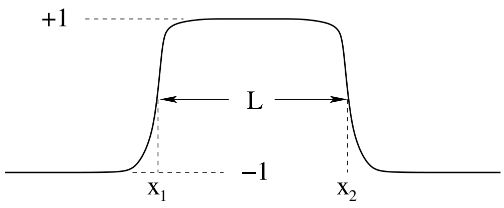

Figure 7.8: A single domain with magnetization close to +1 in a background where the magnetization is close to −1.

only the smallest domain in the system merges with its two nearest neighbors in a single update state. This extremal picture then provides a natural way to determine the domain dynamics.

To understand the origin of the slow domain growth, consider a single large domain of length $L = x_2 - x_1$ in which the magnetization is close to +1. The domain is immersed in a sea with the magnetization close to −1 (Fig. 7.8). The two interfaces of this bubble consist of a kink at $x = x_1(t)$ and an antikink at $x = x_2(t) = x_1 + L$. If L is much larger than the width of each interface, which is a good approximation at long times, the kink and antikink are nearly independent. Under this assumption, the spatial dependence of the order parameter would simply be, using Eq. (7.24),

$$m(x,t) \approx \tanh(x - x_1(t)) - \tanh(x - x_2(t)) - 1. \tag{7.59}$$

Let's estimate how the interfaces move in this kink/antikink domain profile. Substituting the profile (7.59) into the TDLG equation (7.2) and keeping only the lowest-order terms, we find that asymptotically

$$\dot{x}_1 = -\dot{x}_2 \approx e^{-2(x_2 - x_1)}. \tag{7.60}$$

Consequently the length L of the domain shrinks according to

$$\dot{L} \approx -2e^{-2L}, \tag{7.61}$$

which leads to the domain shinking logarithmically with time.

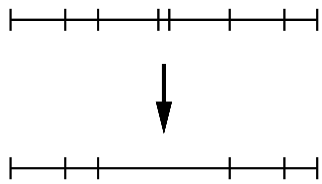

Figure 7.9: Extremal dynamics. The shortest domain merges with its two neighbors.

This logarithmic shrinking has a profound consequence for the evolution of an array of domains of different lengths in one dimension. In the long-time limit where all the domains have significant lengths, Eq. (7.61) shows that the smallest domain in the system shrinks orders of magnitude more quickly than the next smallest domain. In the long-time limit, the order in which domains merge with their neighbors therefore becomes deterministic. This length ordering leads to the following simple extremal dynamics algorithm for domain evolution by the TDGL equation: (i) pick the smallest domain and merge it with its two nearest neighbors; (ii) repeat *ad infinitum* (Fig. 7.9).

The domain length distribution

We now study the evolution of the domain length distribution by this process of merging the shortest current domain with its two neighbors. For simplicity, we assume that the total initial magnetization vanishes, so that that the average length of domains of positive and negative magnetization are equal. The coarsening of this system by the extremal dynamics resembles the cluster dynamics discussed in Sec. 6.5, and the theoretical analysis of the two processes are quite similar. However, in extremal dynamics, the physical time is not a fundamental variable; instead, the length of the shortest domain plays the role of the time in the master equation.

Our goal is to solve for $c(x,s)$, the density of domains of length x when the shortest domain has length s. We choose the initial domain lengths from a continuous distribution so that each domain has a distinct length. The total density of domains is $\rho = \int_s c(x,s)\,dx$ and by definition $\int_s^\infty x\,c(x,s)\,dx = 1$. Let's first show how the shortest domain plays the role of a time-like variable. When the shortest domain has length s, suppose that a certain number of mergings occur so that all domains with lengths in the range $(s, s+\Delta s)$ merge with their neighbors so that the length of the shortest domain increases from s to $s+\Delta s$. The density of the domains in this length range is $c(s,s)\Delta s$. Since three domains are lost and one is gained in each merger, $\rho(s+\Delta s) = \rho(s) - 2c(s,s)\Delta s$. Thus the domain density obeys

$$\frac{d\rho}{ds} = -2c(s), \tag{7.62}$$

with the minimal length s playing the role of time.

The master equation for the domain length distribution may now be written in terms of this time-like variable. When the length of the shortest domain increases from s to $s+\Delta s$, the length distribution $c(x,s)$ changes as follows:

$$c(x,s+\Delta s) - c(x,s) = \left[-2\,\frac{c(x,s)}{\rho} + \Theta(x-3s)\int_s^{x-2s} \frac{c(y,s)}{\rho}\frac{c(x-s-y,s)}{\rho}\,dy\right] c(s,s)\Delta s. \tag{7.63}$$

The first term on the right accounts for the loss of a domain of length x due to its merging. the factor of 2 stems from the fact that a domain of length x can be either to the left or to the right of the minimal domain. The second term accounts for the gain of a domain of length x due to the merging of three domains of lengths s, y, and $x-s-y$. The Heaviside step function $\Theta(x-3s)$ enforces the condition that when the smallest domain has length s, the smallest domain that can be created by merging must have length equal to at least $3s$. The last factor $c(s,s)\Delta s$ counts the number of merging events that occur as the minimal size increases from s to $s+\Delta a$.

A remarkable feature of extremal evolution is that if the domains are initially uncorrelated, they remain uncorrelated at all times because the merging of domains do not affect their neighbors, nor are they affected by their neighbors. Therefore the domain length distribution evolves according to the exact equation

$$\frac{dc(x,s)}{ds} = c(s,s)\left[-2\,\frac{c(x,s)}{\rho} + \Theta(x-3s)\int_s^{x-2s} \frac{c(y,s)}{\rho}\frac{c(x-s-y,s)}{\rho}\,dy\right] \tag{7.64}$$

for $x > s$. At this point, it is again convenient to introduce the normalized length density $P(x,s) = c(x,s)/\rho$ whose governing equation includes only the gain term:

$$\frac{dP(x,s)}{ds} = \Theta(x-3s)P(s,s)\int_s^{x-2s} P(y,s)P(x-s-y,s)\,dy. \tag{7.65}$$

Let's now investigate the asymptotic behavior of the domain length distribution. The ever-growing minimal domain length s defines a basic scale, and we postulate that s is the only length scale in the long time limit. Thus we assume that $P(x,s)$ approaches the scaling form

$$P(x,s) \simeq s^{-1}\Phi\left(xs^{-1}\right) \tag{7.66}$$

as $s \to \infty$, where the prefactor is fixed by the normalization condition $\int_1^\infty P(x,s)\,dx = 1$. As a result, the scaling function must satisfy the normalization condition $\int_1^\infty dz\,\Phi(z) = 1$. Substituting the scaling ansatz for $P(x,s)$ into the master equation (7.65), the scaling function obeys the nonlinear integro-differential equation

$$z\frac{d\Phi(z)}{dz} + \Phi(z) + \Theta(z-3)\Phi(1)\int_1^{z-2} \Phi(y)\Phi(z-1-y)\,dy = 0. \tag{7.67}$$

Given that the master equation contains a convolution integral, it is natural to express the master equation in the Laplace domain. Hence introduce the Laplace transform $\phi(p) = \int_1^\infty \Phi(z)e^{-pz}dz$; here we use the lower limit of 1 because the convolution has this same lower limit. Multiplying (7.67) by e^{-pz} and integrating by parts, the Laplace transform obeys the ordinary differential equation

$$p\frac{d\phi}{dp} = -\Phi(1)\left(1-\phi^2\right)e^{-p}, \tag{7.68}$$

with the boundary condition $\phi(0) = 1$. Expanding $\phi(p) = 1 + p\phi'(0)$ on the right hand side and evaluating the equality at $p = 0$ yields the normalized density of the shortest domains $\Phi(1) = 1/2$. Asymptotically, the density of the shortest domains is

$$P(s) \simeq (2s)^{-1}. \tag{7.69}$$

Substituting this value into (7.68) and solving the explicit equation yields the Laplace transform

$$\phi(p) = \tanh\left[\mathrm{Ei}\,(p)/2\right], \tag{7.70}$$

in terms of the exponential integral $\mathrm{Ei}\,(x) = \int_x^\infty u^{-1}\exp(-u)du$.

The average domain length, $\langle x\rangle \simeq \langle z\rangle s$, follows from the small-argument behavior $\phi(p) \cong 1 - p\langle z\rangle$ and the asymptotic properties of the exponential integral[1]

$$\langle x\rangle \simeq 2e^\gamma\, s. \tag{7.71}$$

The ratio between the average domain length and the minimal domain length approaches the constant $2e^\gamma = 3.562144$. The conservation law $\rho\langle x\rangle = 1$ then gives the total domain density $\rho \simeq \frac{1}{2}e^{-2\gamma}s^{-1}$. Indeed, the density satisfies (7.62) $d\rho/ds = -2P(s)\rho \simeq \rho/s$.

Extremal properties of the domain distribution can be evaluated directly from the integro-differential equation (7.67). In the length range $1 < z < 3$, the integral drops out. The scaling function obeys the differential equation $z\frac{d}{dz}\Phi(z) = -\Phi(z)$ with the boundary condition $\Phi(1) = 1/2$, so

$$\Phi(z) = (2z)^{-1}, \qquad 1 \le z \le 3. \tag{7.72}$$

Interestingly, the normalized domain density becomes time-independent, $P(x,s) \to (2x)^{-1}$, in the (time-dependent) range $s < x < 3s$.

add exponential tail of distribution

The most remarkable aspect of this process is that it is exactly soluble. Often, this is the case in extremal dynamics because they are deterministic. The source of randomness is solely in the initial conditions and correlations are not generated by the dynamics, in contrast with stochastic evolution.

The scaling analysis employed effectively resets the length of shortest domain to one after each merger. The similarity solution can be viewed as a *fixed-point* of this renormalization procedure. This technique is sometime termed *real space renormalization* or *strong disorder renormalization*.

Persistence

More subtle characteristics of the domain evolution may be addressed by exploiting the fact that domains are uncorrelated. One may ask: what is the probability that a given spin maintained its initial value throughout the evolution. Persistence elegantly probes the history.

Let $Q(x)$ be the average length of persistent regions in a domain of length x. In a merger between domains of lengths y, s, and $x-s-y$, the average persistence length of the emerging domain is $Q(y) + Q(x-s-y)$. Therefore,

$$\frac{d}{ds}\left[P(x)Q(x)\right] = \Theta(x-3s)P(s)\int_s^{x-2s} P(y)P(x-1-y)[Q(y)+Q(x-s-y)]dy. \tag{7.73}$$

The persistence probability $P_{\rm per}(s) = \langle x\rangle^{-1}\int_s P(x)Q(x)dx$ must be larger than s^{-1} but smaller than one. Thus, we anticipate the algebraic behavior, $P_{\rm per}(s) \sim s^{-\theta}$ with $0 < \theta < 1$. Consistent with this behavior is the scaling form

$$P(x)Q(x) \simeq s^{-\theta}\Psi(xs^{-1}). \tag{7.74}$$

[1]For small-x, $\mathrm{Ei}\,(x) \simeq -\gamma - \ln x$ with $\gamma = 0.577215$ the Euler constant.

Self-Similarity

There is a fundamental difference between the scaling forms underlying the length distribution (7.66) and the persistence distribution (7.74). The former is written based on dimensional analysis, namely, consistency with the known integrals $\int_s dxP(x) = 1$ and $\int_s dxxP(x) \sim s$. However, the latter involves the yet unknown parameter θ. It reflects the partial *a priori* knowledge, $\int_s dxxP(x)Q(x)/\int_s P(x)Q(x) \sim s$. Determination of the unknown parameter θ requires us to solve for the family of scaling solutions and then impose a self-consistency criteria to determine the physical solution. While scaling properties of the domain length distribution follow from dimensional analysis, this is not the case for persistence. These two types of self-similarity functions are distinguished as scaling solutions of the *first* and the *second* kind, respectively.

The scaling function satisfies the *linear* integro-differential equation

$$x\frac{d}{dx}\Psi(x) + \theta\,\Psi(x) + \Theta(x-3)\int_1^{x-2}\Phi(y)\Psi(x-1-y)dy. \tag{7.75}$$

The identity $2\Phi(1) = 1$ was used to simplify the last term. The Laplace transform $\psi(p) = \int_1 dze^{-pz}$ couples to the known function $\phi(p)$ via the *linear* differential equation

$$p\frac{d}{dp}\psi(p) + (1-\theta)\,\psi(p) = -e^{-p}\left[\Psi(1) - \phi(p)\psi(p)\right]. \tag{7.76}$$

The solution is as follows

$$\psi(p) = \frac{\Psi(1)}{p}\int_p^\infty \frac{q^{-\theta}\cosh^2[\mathrm{Ei}(q)/2]}{p^{-\theta}\cosh^2[\mathrm{Ei}(p)/2]}\,e^{-q}\,dq. \tag{7.77}$$

The exponent θ is obtained from the small-p behavior. On the one hand, from the definition of the Laplace transform $\psi(p) = M_0 - M_1 p + \cdots$ with the moments $M_n = \int \Psi(z)z^n dz$. On the other hand, the explicit solution reads

$$\psi(p) = \frac{\Psi(1)}{\theta}\left[1 + f(\theta)p^\theta + \mathcal{O}(p)\right] \tag{7.78}$$

The prefactor $f(\theta)$ is evaluated from (7.84) using $\mathrm{Ei}\,(p) - \ln p \cong -\gamma - \sum_{n=1}(-p)^n/[n\cdot n!]$. A tedious calculation yields

$$f(\theta) = e^\gamma\int_0^\infty dq\,q^{-\theta}e^{-q}\,\left\{(1-q-e^{-q})\exp[\mathrm{Ei}(q)] + 2\theta + \theta\exp[-\mathrm{Ei}(q)]\right\}. \tag{7.79}$$

To match the two expressions, we impose $f(\theta) = 0$. Thus, only one of the family of solutions (7.84) is physical. Numerical evaluation of the integral yields the persistence exponent; the persistence probability decays as

$$P_{\rm per}(s) \simeq s^{-\theta}, \qquad \theta = 0.175075. \tag{7.80}$$

The exponent is quite small, so the decay is slow.

Clearly, this exponent can not be obtained from dimensional analysis and it follows from a self-consistency requirement. Typically, such requirements are discerned from extremal properties of integral transforms (Fourier, Laplace, or Mellin).

Autocorrelation

Another measure of history is the autocorrelation function, $A(s) = \langle\sigma(x,0)\sigma(x,s)\rangle$, with $\sigma(x,s)$ the spin-value at position x at "time" s. Let the average autocorrelation for a domain of length x be $A(x)$. As domains merge, the average autocorrelation is $A(y) - A(s) + A(x-1-y)$ because the minimal domain flips. Hence, the master equation is

$$\frac{d}{ds}\left[P(x)A(x)\right] = \Theta(x-3s)P(s)\int_s^{x-2s} P(y)P(x-1-y)[A(y) - A(s) + A(x-s-y)]dy. \tag{7.81}$$

We assume that the autocorrelation, $A(s) = \langle x\rangle^{-1}\int_s A(x)P(x)dx$, decays algebraically with the domain length, $A(s) \simeq s^{-\lambda}$, or alternatively, the scaling behavior $P(x)A(x) \simeq s^{-\lambda}\psi(xs^{-1})$. The scaling function satisfies the linear integro-differential equation

$$x\frac{d}{dx}\Psi(x) + \lambda\,\Psi(x) + \Theta(x-3)\int_1^{x-2}\left[\Psi(y) - \Psi(1)\Phi(y)\right]\Phi(x-1-y)dy. \tag{7.82}$$

The Laplace transform obeys the linear ordinary differential equation

$$p\frac{d}{dp}\psi(p) + (1-\lambda)\,\psi(p) = -e^{-p}\left[\Psi(1)(1+\phi^2(p)) - \phi(p)\psi(p)\right]. \tag{7.83}$$

Solving this equation, the Laplace transform is

$$\psi(p) = \frac{\Psi(1)}{p}\int_p^\infty \frac{q^{-\lambda}\cosh[\mathrm{Ei}\,(q)]}{p^{-\lambda}\cosh^2[\mathrm{Ei}\,(p)/2]}\,e^{-q}\,dq. \tag{7.84}$$

Expanding the Laplace transform, $\psi(p) \cong \frac{\Psi(1)}{\lambda}\left[1 + f(\lambda)p^\lambda + \mathcal{O}(p)\right]$, the exponent λ is the root of the equation $f(\lambda) = 0$ with

$$f(\lambda) = e^\gamma\int_0^\infty dq\,q^{-\lambda}e^{-q}\left\{(1-q-e^{-q})\exp[\mathrm{Ei}\,(q)] + \lambda\exp[-\mathrm{Ei}\,(q)]\right\}. \tag{7.85}$$

The autocorrelation exponent is found numerically

$$A(s) \simeq s^{-\lambda}, \qquad \lambda = 0.600616. \tag{7.86}$$

The primary domain characteristic, the length distribution, obeys a closed non-linear equation. Secondary characteristics such as persistence and autocorrelation involve a linear equation that couples to the domain distribution. While the scaling properties of the primary distribution follow from conservation laws, the scaling properties of secondary characteristics involve the entire form of the domain distribution. This situation is generic in irreversible processes. Primary statistics are robust, universal. Secondary statistics, coupled to the primary statistics, are fragile, non-universal.

References

1. I. M. Lifshitz and V. V. Slyozov, Zh. Eksp. Teor. Fiz. **35**, 479 (1959).

2. D. S. Fisher and D. A. Huse, Phys. Rev. B **38**, 373 (1988).

3. M. C. Cross and P. C. Hohenberg, Rev. Mod. Phys. **65**, 851 (1993).

4. A. J. Bray, Adv. Phys. **43**, 357 (1994).

5. A. J. Bray and B. Derrida, Phys. Rev. E **51**, 1633 (1995).